Dynamic Initialization of Fixed-speed Pump as Turbines Using Unified Newton-Raphson power-flow Approach

Pattiya Thongkruer*, Pichai Aree

Power System and Electrical Machine Research Group, Department of Electrical Engineering, Thammasat University, Pathumthani, Thailand

Abstract

Fixed-speed pump-as-turbine generators (FSPATs) have been more utilized in grid-linked small hydro power plants (SHPs) for several years. Their initializations for power-system dynamic simulations can be applied using a traditional power-flow approach; however, this approach leads to an inevitable reactive-power difference between power-flow result and the actual one required by FSPAT. To overcome this problem, an accurate power-flow initialization of FSPAT is needed. Nervetheless, FSPAT initialization has not yet been addressed. Hence, in this research, an unified Newton-Rapshon (NR) approach along with pump-as-turbine characteristic curves is employed for precise dynamic initialization of the FSPAT. The power-flow solution with FSPAT is demonstrated through 4 buses network system. Moreover, an efficiency of the proposed NR algorithm is investigated using IEEE-30 bus network with a large group of SHPs. The results expose that the proposed algorithm not only provides a precise steady-state initialization without the reactive power discrepancy but also keeps the quadratic convergence of NR method.

Keywords: pump-as-turbine; Newton-Raphson approach; dynamic initialization; hydro power plant

1. Introduction

Nowadays, many small-scale hydro power plants (SHPs) are promising for electricity production in remote areas due to environment-friendly, small construction facilities, and low running cost. SHP is usually a run-of-river plant which does not require a large reservoir for power generation. It can supply the power in the range up to 2 MW [1]. Because the high-cost conventional turbines are not suitable for SHP application, pump as turbine (PAT) is potentially considered as a cost-effective alternative solution for SHPs [2].

In recent years, it has been reported that an interest in PAT application in SHP has raised due to many advantages over the conventional turbines [3]. Most of PATs can be categorized into fixed and variable speeds. Fixed-speed pump as turbine (FSPAT) is often equipped with an induction generator based on a squirrel-cage rotor type (SCIG). It performs within a limited speed range. Because most of the SCIGs integrated with the FSPAT are typically connected with main power grid for more efficient operation, they may affect the dynamics of power system. Hence, including the FSPAT into power-system dynamic assessment has become increasingly important. Because, the power-system dynamic simulation mostly requires an accurate steady-state initial condition, a proper dynamic initialization of FSPAT is mainly addressed in this paper. Nowadays, the most promising method ordinarily used for initializing SCIG is on the basis of power-flow model. In general practice, the SCIG is represented as normal PQ load allowing that active and reactive powers of SCIG are inputted as the specified quantities and kept constant until the power-flow computation is finished. However, this approach is not straightforward to give an accurate dynamic initialization of network including the SCIGs due to an inevitable reactive-power mismatch between power-flow converged result and the one that is really consumed by the SCIG (computed using the converged voltage). This discrepancy is traditionally solved adding a shunt compensator into the SCIG's terminal bus [4]. This current initializing method, is widely employed in some commercial power-system software tools [5,6].

It has been reported that the artificial admittance caused by unsuitable initialization leads to an incorrect

* Corresponding author. Tel.: +66-95-739-8134
E-mail address: pattiya.thon@dome.tu.ac.th

dynamic assessment, especially for the case of weak grid connection, when the SCIG's reactive powers are very sensitive to their bus voltages [4]. To eliminate the undesired artificial admittance, sequential and unified power-flow approaches can be applied. Recently, several researches have been presented approaches for initializing fixed-speed wind generator (FSWG) based on both initializing approaches. However, based on the literature review, the unified approach gives a better way for computing the steady-state solution of FSWG because it yields a quadratic convergence [7-9]. In [8-9], the unified method is put forward to calculate the steady-state operating point of FSWGs. The study results show that initialization of FSWG directly from aerodynamic power coefficient can yield a precise steady-state solution of FSWGs, completely correlating with their actual dynamic behaviour.

So far, the dynamic initialization of FSPAT has not been yet reported in the literature. To eliminate the undesired reactive-power mismatch, an accurate initialization of FSPAT is required. Hence, this paper presents a precise initialization of FSPATs using the unified method. The Newton-Raphson (NR) algorithm is extended to solve the network and FSPAT variables simultaneously in order to eradicate the reactive-power mismatch and maintain convergence manner. Moreover, characteristic curves of FSPAT are incorporated into the proposed NR method to get the power-flow solution which fully relates with the actual behaviour of the FSPAT. Besides, the convergent characteristic of the proposed NR algorithm is investigated when a great number of FSPATs are incorporated into IEEE-30 bus power network.

2. **SCIG and Pump as turbine Models**

2.1 SCIG model

In this paper, instead of using a common T equivalent circuit model of SCIG, an inverse-Γ model in [9] as shown in Fig. 1 is employed. Because the inverse-Γ model only consists of an internal complex emf (E'), it is suitable to be incorporated into power-flow model. According to Fig. 1, the air-gap power (Pag) can be written in per-unit expression as,

$$P_{ag}^{*} = -\left\{ \left(X_{rr}/X_m \right)^2 \left(s/R_r \right) E'^2 \right\} \quad (1)$$

$$P_{ag}^{\bullet} = -\frac{VE'}{R_s^2 + X'^2} \begin{Bmatrix} \left(R_s \cos\left(\theta - \theta'\right) \right) \\ -X' \sin\left(\theta - \theta'\right) \\ -R_s E'/V \end{Bmatrix} \quad (2)$$

Where the stator and rotor resistances as well as transient reactance are denoted as Rs, Rr and X', respectively. The rotor self-reactance (Xrr) is a total of mutual reactance and rotor leakage (Xm+Xlr). It should be remarked that the negative signs applied to (1) and (2) are regarded as injected quantities.

It has been reported that the artificial admittance caused by unsuitable initialization leads to an incorrect

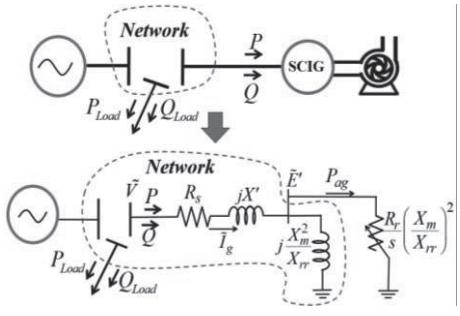

Fig. 1 equivalent circuit model of SCIG (Inverse-Γ)

2.2 Pump-as-Turbine model

Typically, the mechanical power generated from the PAT for a given head (h) in meter, water flow rate (q) in m3/s and efficiency (η), can be expressed in term of per unit as, 12

$$P_{pat} = \eta \rho g q h / S_{base} \quad (3)$$

Where ρ and g represent water density and gravity, respectively. The efficiency (η) and flow rate (q) can be calculated by fitting polynomial regression to the available performance data in [10] as,

$$\eta = \alpha_6 N_{pat}^6 + \alpha_5 N_{pat}^5 + \ldots + \alpha_0 \quad (4)$$

$$q = \beta_6 N_{pat}^6 + \beta_5 N_{pat}^5 + \ldots + \beta_0 \quad (5)$$

where N_{pat} is given by

$$N_{pat} = 120 f (1-s)/p \quad (6)$$

The coefficients α_1-α_S and β_1-β_S in (Q) and (R) can be found via fitting S order polynomial regression to the available performance data. Thus, by knowingthe rotor speed, the corresponding efficiency and flow rate of PAT can be determined from (Q) and (R). According to (S), the rotor speed (kpat) of PAT can be calculated from slip (s), frequency (f), and number of pole (p) of SCIG, respectively. Commonly, the turbine-shaft torque and air-gap power are equal in per-unit quantity. Thus, the shaft torque (Tpat) can be written in per-unit term by,

$$T_{pat} = P_{ag} = P_{pat} \big/ (1-s) \qquad (7)$$

3. Initialization Power-flow Model

The proposed NR power-flow algorithm for finding steady-state operating point of FSPAT is addressed in this section. Since the variables of SCIG such as slip (s), internal emf (E') and angle (θ') are incorporated as iterative variables, the mismatch function can be written by [11],

$$\mathbf{f}(\mathbf{x}) = -\mathbf{J}(\mathbf{x})\Delta\mathbf{x} \qquad (8)$$

where

$$\mathbf{f(x)} = \begin{bmatrix} \mathbf{f}_1(\mathbf{x}) = \mathbf{P}_{1\text{-n}}^{\text{cal}} - \mathbf{P}^{\text{sche}} \\ \mathbf{f}_2(\mathbf{x}) = \mathbf{P}_{1\text{-m}}^{\text{cal}} - \mathbf{P}_{\text{ag}}^{*} \\ \mathbf{f}_3(\mathbf{x}) = \mathbf{Q}_{1\text{-n}}^{\text{cal}} - \mathbf{Q}^{\text{sche}} \\ \mathbf{f}_4(\mathbf{x}) = \mathbf{Q}_{1\text{-m}}^{\text{cal}} - \mathbf{Q}_{\text{ag}}^{\text{sche}} \\ \mathbf{f}_5(\mathbf{x}) = \mathbf{T}_{\text{pat}} - \mathbf{P}_{\text{ag}}^{\bullet} \end{bmatrix} \qquad (9)$$

$$\mathbf{x} = \begin{bmatrix} \boldsymbol{\theta} & \boldsymbol{\theta}' & \mathbf{V} & \mathbf{E}' & \mathbf{s} \end{bmatrix}^T \qquad (10)$$

$$\mathbf{J(x)} = \begin{bmatrix} \mathbf{J}_{\text{con}}(\mathbf{x}) + \mathbf{J}_{\text{pat}}(\mathbf{x}) \end{bmatrix} \qquad (11)$$

The iteration formula of NR algorithm is given by,

$$\mathbf{x}^{(r+1)} = \mathbf{x}^{(r)} + \Delta\mathbf{x} \qquad (12)$$

n (9), the superscripts cal and sche denote calculated and scheduled quantities, respectively. The subscripts 1-n and 1-m refer to the whole numbers of network and SCIG's internal buses. The proposed NR algorithm can be modified as follows,

1. Specifying the designed head (h) of FSPAT and its iterative variables.
2. Calculating SCIG initial slip using the rated terminal bus voltage (1 pu.) by solving the steady-state power equilibrium in (13) as presented in next section.
3. Calculating flow rate (q), efficiency (η) of FSPAT in (4) and (5) as well as the initial internal emf magnitude (E') using the inverse-Γ model in Fig. 1.
4. Incorporating SCIG's impedance encircled by the dashes line as shown in Fig. 1 into network admittance matrix.
5. Calculating mismatch function in (9). A list of relevant equations for $\mathbf{f_2(x)}$ and $\mathbf{f_5(x)}$ are displayed in Table 1. The reactive power ($\mathbf{Q}_{\text{ag}}^{\text{sche}}$) in $\mathbf{f_4(x)}$ is set to zero since internal bus of SCIG has no injected reactive power.
6. Computing the conventional $\mathbf{J_{con}(x)}$ and PAT $\mathbf{Jpat(x)}$ Jacobian matrixes, which can be derived from differentiating the mismatch function in (9).

Table 1. Initialization of FSPAT and its mismatch function

	Variable and function
Input quantity	h
Output quantity	P, Q, V, θ, s, q, η
$\mathbf{f_2(x)}$	$\mathbf{P}_{\text{ag}}^{\text{cal}}$- Eq. (1)
$\mathbf{f_5(x)}$	Eq. (7) – Eq. (2)

4. SCIG's slip Initialization

Before the initialization process starts, the terminal bus voltage magnitudes and phase angles of all SCIG buses are set to 1 pu. and 0 radian, respectively. Referred to Fig. 1, the slip (s) can be computed by,

$$P - I_g^2 R_s - P_{ag} = 0 \qquad (13)$$

When expressed in per-unit quantities the active power (P) and input current (I_g) related to SGIG's voltage magnitude (V) and slip (s) can be revealed by,

$$P = \left(V^2 R_{mot}\right) \big/ \left(R_{mot}^2 + X_{mot}^2\right) \qquad (14)$$

$$I_g = (V) \big/ \sqrt{\left(R_{mot}^2 + X_{mot}^2\right)} \qquad (15)$$

where,

$$R_{mot} = R_s + \frac{s\left(R_r X_m^2\right)}{\left(R_r^2 + s^2 X_{rr}^2\right)} \qquad (16)$$

$$X_{mot} = X' + \frac{R_r^2 X_m^2}{X_{rr}\left(R_r^2 + s^2 X_{rr}^2\right)} \qquad (17)$$

5. Power-flow Initialization

The power-flow initialization of FSPAT is presented in this section. The benchmark system in [9] and 250 HP SCIG with their parameters given in Fig. 2 are employed. The available

performance data of FSPAT taken from [10] are listed in Appendix A. It should be noted that all parameters shown in Fig. 2 are based on 10 MVA.

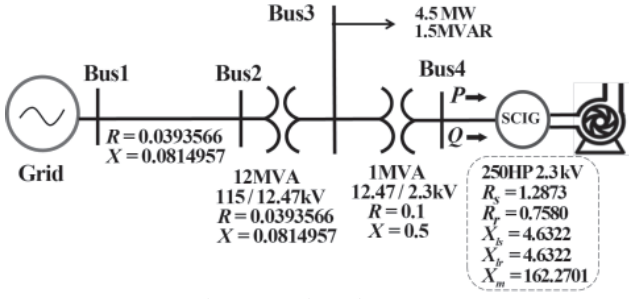

Fig. 2 Benchmark system

In this study, 6th degree polynomial equations in (4) and (5), obtained by means of fitting curve regression to the efficiency and flow rate data, are applied for the unified power-flow calculation in order to get the steady-state solution in full correlation with the characteristic curves of PAT.The coefficients αN-α6 and βN-β6 shown in (4) and (5) are given in Appendi• B. Fig. P demonstrates comparisons between the actual and estimated efficiency and flow rate curves. It can be observed that a change in the speed of FpPAT (rpm) is completely related to its efficiency and flow rate. Before starting the power-flow calculation, the water head VM.V2m, regarded as input quantity of FpPAT, is firstly specified. Then, the p`Id'̀s slip is solved using the rated voltage (N.M pu.) to find the magnitude of internal emf (bD) regarded as an initial value. The phase angle (θ') is set to zero. After the power-flow computation is done with a given tolerance of 10-12 in four iterations, the obtained voltages, phase angles, active and reactive powers of all buses are displayed in Fig. 4. Also, the SCIG's air-gap power, rotor speed, internal-bus emf, phase angle as well as flow rate and efficiency of FSPAT are located at the final row. These quantities are immediately received after the converged solution arrives. Moreover, the obtained speed of SCIG are precisely matched with the converged flow rate and efficiency of FSPAT becuase they are automatically updated at every iteration of plow-flow process. For instance, referred to Fig. 4 in final row, the converged SCIG's speed, flow rate and efficiency of FSPAT are 1824 rpm, 0.2286 m3/s and 0.8464, respectively. Similarly, referred to Fig. 3, the PAT characteristic curves provide the same value of flow rate and efficiency when the PAT operates at 1824 rpm. Hence, it is can be said that the converged power-flow solution is fully related to the obtained flow rate and efficiency characteristic curves of FSPAT.

In addition, the computational accuracy of the study results obtained from the proposed algorithm is verified. The converged active and reactive powers of SCIG bus as shown Fig. 5 (-0.1657MW + j0.09MVAR) are used as the fixed inputs to re-calculate the power-flow solution via the conventional approach, starting from the rated voltage (1 pu.). After applying the conventional power-flow calculation, the converged results are displayed in Fig. 5. As expected, the converged voltages and powers

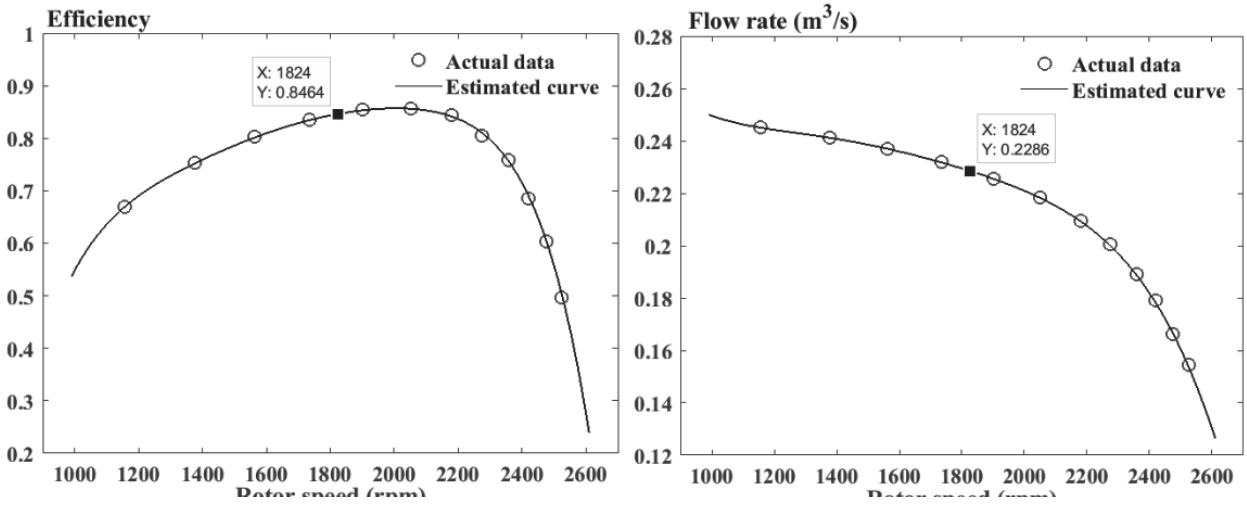

Fig. 3 Characteristic curves; efficiency curve (left hand); flow rate curve (right hand)

both proposed and conventional algorithms are exactly the same, ensuring the numerical correctness of the computational results. In other words, this proposed initializing method fully yields the exact reactive power demand of SCIG. Hence, no artificial admittances are added for compensating the difference between the schedule and actual reactive power when the FSPAT is included in initializing dynamic simulation. Besides, it can be observed that the computational time between the proposed and conventional methods are not different.

6. Convergence Test

In this section, the computational efficiency of the proposed algorithm is investigated with IEEE-30 bus test network including 18 groups of small-scale hydro power plants. A practical 8 bus in SHP is employed as shown in Fig. 6. Due to additional buses arisen from 18 of individual SHP network and SCIG internal bus, the original IEEE-30 bus system expanded from 30 to 264 buses. The 250 HP SCIGs are incorporated into these SHPs. All FSPATs are specified with the water head (h) of 90.92 m.

After steady-state solution of tested network is converged, the mismatch versus a number of iterations is displayed in Fig. 7. The normalized mismatch of the original IEEE-30 bus network is also plotted for making comparison. It can be observed that the power mismatch of IEEE-30 bus network with individual 8bus SHP into 18 assigned load buses is inconsiderably deviated from that of the original network. Hence, it is confirmed that this initializing power-flow method is very effective because the mismatch convergence characteristic still

Proposed method

MvaBase : 10.00 Tolerance : 1e-12

Total MW losses : 0.1064 Total MVAR losses: 0.3849

Total time : 0.047 sec.

Bus	Voltage	Angle	------Load------		---Generation---	
No.	Mag.	Degree	MW	MVAR	MW	MVAR
1.0000	1.0500	0	0	0	4.4361	1.9423
2.0000	1.0316	-1.8694	-0.0000	0.0000	0	0
3.0000	1.0012	-3.4817	4.5000	1.5000	0	0
4.0000	0.9983	-2.9553	0.0000	-0.0000	0	0
5.0000	0.9515	6.9215	-0.0000	-0.0000	0.1703	0

Con Bus	Int Bus	HP	Vmot p.u.	Angle Degree	P MW	Q MVar	Pag MW	Speed rpm	q (m^3/s)	eff
4	5	250	0.9983	-2.9553	-0.1657	0.0900	-0.1703	1824	0.2286	0.8464

Fig. 4 Power flow solution using proposed power-flow algorithm

Conventional method using NR algorithm

MvaBase : 10.00

Tolerance : 1e-12

Total MW losses : 0.1018

Total MVAR losses: 0.3523

Total time : 0.032 sec.

Bus	Voltage	Angle	------Load------		---Generation---	
No.	Mag.	Degree	MW	MVAR	MW	MVAR
1.0000	1.0500	0	0	0	4.4361	1.9423
2.0000	1.0316	-1.8694	0	0	0	0
3.0000	1.0012	-3.4817	4.5000	1.5000	0	0
4.0000	0.9983	-2.9553	-0.1657	0.0900	0	0

Fig. 5 Power flow solution using conventional power-flow algorithm

preserves in quadratic manner.

In this section, the computational efficiency of the proposed algorithm is investigated with IEEE-30 bus test network including 18 groups of small-scale hydro power plants. A practical 8 bus in SHP is employed as shown in Fig. 6. Due to additional buses arisen from 18 of individual SHP network and SCIG internal bus, the original IEEE-30 bus system expanded from 30 to 264 buses. The 250 HP SCIGs are incorporated into these SHPs. All FSPATs are specified with the water head (h) of 90.92 m.

After steady-state solution of tested network is converged, the mismatch versus a number of iterations is displayed in Fig. 7. The normalized mismatch of the original IEEE-30 bus network is also plotted for making comparison. It can be observed that the power mismatch of IEEE-30 bus network with individual 8bus SHP into 18 assigned load buses is inconsiderably deviated from that of the original network. Hence, it is confirmed that this initializing power-flow method is very effective because the mismatch convergence characteristic still preserves in quadratic manner.

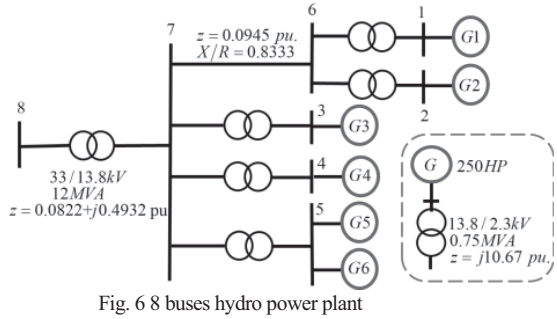

Fig. 6 8 buses hydro power plant

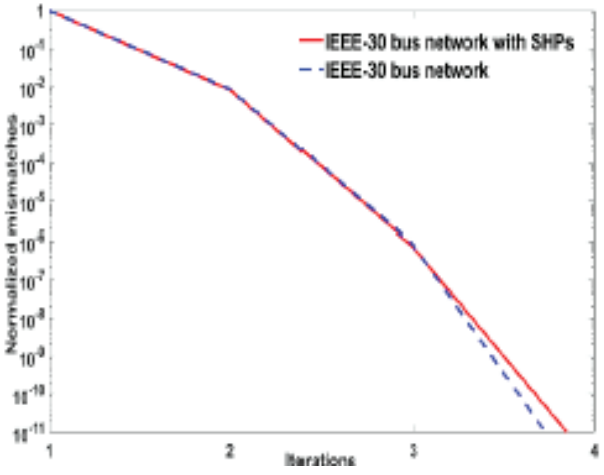

Fig. 7 Mismatch characteristics

7. Conclusion

This research presents the extended NR algorithm to find the accurate steady-state operating points required for power-system initialization including FSPAT. The variables of system network and FSPAT are incorporated into the power- flow mismatch function and Jacobian in order to solve them in the unified manner. An incorporation of the FSPAT characteristic curves into proposed algorithm yields precise steady-state solutions, fully correlating with the actual performance curves of FSPAT. Also, the proposed initializing method is demonstrated and verified using 4 buses system. The study shows that the exact amount of reactive power of FSPAT is directly obtained in correlation with the converged bus voltage. So, the proposed algorithm is superior to the tradition power-flow initialization approach, commonly applied in the commercial software packages due to absolutely eradicating the need of fictitious admittance for compensating the reactive-power discrepancy. Moreover, efficiency of the initialization approach proposed in this paper is presented using IEEE 30 bus network with several groups of small-scale hydro power plant. The results expose that convergent property of the proposed NR algorithm is still remained quadratic style.

References

[1] Nababan, S., Muljadi, E., & Blaabjerg, F. (2012, 25-28 June 2012). An overview of power topologies for micro-hydro turbines. Paper presented at the 2012 3rd IEEE International Symposium on Power Electronics for Distributed Generation Systems (PEDG).

[2] Jain, S. V., & Patel, R. N. (2014). Investigations on pump running in turbine mode: A review of the state-of-the-art. Renewable and Sustainable Energy Reviews, 30, 841-868.

[3] Williams, A. A. (1996). Pumps as turbines for low cost micro hydro power. Renewable Energy, 9(1), 1227-1234.

[4] Nandigam, K., & Chowdhury, B. H. (2004, 6-10 June 2004). Power flow and stability models for induction generators used in wind turbines. Paper presented at the IEEE Power Engineering Society General Meeting, 2004.

[5] PSS/E 32.0. (Power Technologies Inc., 2009). Program application guide volume II. 21–23.

[6] DSA Tools. (Powertech Labs Inc., British Columbia, Canada, 2011). TSAT model manual. 106.

[7] Cumar, R. J. R., &Jain, A. (2016, 19-21 Dec. 2016). Incorporation of Asynchronous Generators as PQ model in load flow analysis for power systems with wind generation. Paper presented at the 2016 National Power Systems Conference (NPSC).

[8] Castro, L. M., Fuerte-Esquivel, C. R. , et al. (2011). A unified approach for the solution of power flows in electric power systems including wind farms. Electric Power Systems Research, 81(10), 1859-1865.

[9] Aree, P. (2018). Precise dynamic initialisation of

fixed-speed wind turbines under active-stall and active-pitch controls from their aerodynamic power coefficients using unified Newton–Raphson power-flow approach. IET Generation, Transmission & Distribution, 12(1), 9-19.

[10] Alatorre-Frenk, C. (2019). Cost minimisation in micro-hydro systems using pumps-as-turbines.

[11] Machowski, J., et al. (1997). Power System Dynamics and Stability, John Wiley & Sons, England.

Appendix A

Appendix A provides the performance data of PAT with specified water head 90.92 m [10].

Flow rate q (m^3/s)	Efficiency η	Speed N_{pat} (rpm)
0.2450	0.670	1157
0.2412	0.753	1377
0.2369	0.803	1563
0.2319	0.835	1736
0.2256	0.854	1900
0.2184	0.857	2051
0.2096	0.844	2179
0.2004	0.805	2273
0.1891	0.759	2358
0.1792	0.685	2421
0.1662	0.604	2475
0.1546	0.497	2525

Appendix B

Appendix B provides the coefficient of efficiency and flow rate in Fig. 3 and 4

$\alpha_6 = -9.8775\times10^{-19}, \alpha_5 = 1.0043\times10^{-14}, \alpha_4 = -4.2403\times10^{-11},$
$\alpha_3 = 9.5063\times10^{-8}, \alpha_2 = -1.1946\times10^{-4}, \alpha_1 = 8.0173\times10^{-2},$
$\alpha_0 = -21.855$

$\beta_6 = 6.4263\times10^{-21}, \beta_5 = -1.2958\times10^{-16}, \beta_4 = 7.8935\times10^{-13},$
$\beta_3 = -2.2555\times10^{-9}, \beta_2 = 3.3567\times10^{-6}, \beta_1 = -2.5384\times10^{-3}$
$\beta_0 = 1.0206$